

Admittance spectroscopy revisited: Single defect admittance and displacement current

V. G. Karpov^{a)} and Diana Shvydka

Department of Physics and Astronomy, University of Toledo, Toledo, Ohio 43606

U. Jayamaha

First Solar, LLC, 12900 Eckel Junction Road, Perrysburg, Ohio 43551

A. D. Compaan

Department of Physics and Astronomy, University of Toledo, Toledo, Ohio 43606

(Received 1 May 2003; accepted 12 August 2003)

A general approach to semiconductor device admittance spectroscopy analysis is developed, which describes arbitrary defect distributions, and gives the geometrical capacitance limit and the relationship between the measured conductance and capacitance. A single defect capacitance concept is introduced that facilitates the analysis. Special attention is paid to accounting for the role of displacement current, which was overlooked in the preceding work. An experimental verification of the approach is given. © 2003 American Institute of Physics. [DOI: 10.1063/1.1617363]

I. INTRODUCTION

Admittance spectroscopy is one of the major semiconductor diagnostic techniques. It has several modifications,^{1–3} of which the capacitance–voltage ($C-V$) and admittance–frequency ($Y-\omega$) are most known. The $C-V$ profiling tests the spatial charge distribution. Frequency dependent admittance $Y(\omega)$ is generally attributed to defects. Indeed, because in response to the testing ac electric potential, defects change their occupation numbers depending on their relaxation times, they have frequency dependent charge storing ability. In spite of numerous applications, the $Y(\omega)$ data are not fully understood. The interpretation lacks basic concepts that would apply to an arbitrary system/model and discriminate between major features and minor details. For example, the displacement current component is commonly missed in the calculated admittance; the existing models do not contain the geometrical capacitance limit; there is no direct way to estimate the number of contributing defects from the data. In this work we try to put the admittance spectroscopy interpretation on a more solid basis. We introduce a single defect impedance concept, which facilitates the data interpretation, and pay special attention to taking the displacement current into consideration. We derive the formula for admittance that applies to any system, contains the geometrical capacitance limit, and establishes the domains of applicability of the existing models.

Our article is organized as follows. In Sec. II we present an intuitive approach to a single defect capacitance. This approach is substantiated and extended to the case of defect admittance in Sec. III. In Sec. IV we describe how the testing ac electric signal is screened in the system. Section V presents a general formula for defect related integral system admittance. This formula is specified in Sec. VI for the limiting cases of (a) the constant defect density of states, (b)

narrow defect band, and (c) arbitrary defect distribution in the weak screening limit. In Sec. VII we derive the relationship between the admittance and capacitance, which is significantly different from the Kramers–Krönig transformation and has a form specific to defect contributions. Our findings are experimentally verified in Sec. VIII for the case of CdTe photovoltaics.

II. ELEMENTAL DEFECT CAPACITANCE

We start with an intuitive explanation of a single defect capacitance based on the band diagram (Fig. 1) that includes a number of defect levels and band bending caused by external bias or contact potential. In particular, it can represent a Schottky barrier⁴ or part of a $p-n$ junction. Consider a defect level with the energy E_ω below the band edge. A small testing ac voltage $U = U_0 \exp(i\omega t)$ modulates the free-carrier concentration in the proximity of the defect. This can be equally expressed in terms of the local quasi-Fermi level modulation, $\delta E_F = qU$, where q is the electron charge. To begin, we assume the defect relaxation time to be short, $\omega\tau \ll 1$. Then, the defect occupation will adiabatically follow δE_F ,

$$\delta f = (-\partial f / \partial E) \delta E_F = f(1-f) \delta E_F / kT,$$

where $f = \{1 + \exp[(E_F - E)/kT]\}^{-1}$ is the Fermi distribution. The change in occupation number induces the current,

$$j = q \frac{\partial \delta f}{\partial t} = i\omega C_0 U, \quad (1)$$

where, in accordance with Ohm's law, we have introduced the elemental quasistatic ($\omega\tau \ll 1$) defect capacitance

$$C_0 = f(1-f) \frac{q^2}{kT}. \quad (2)$$

^{a)}Electronic mail: vkarpov@physics.utoledo.edu

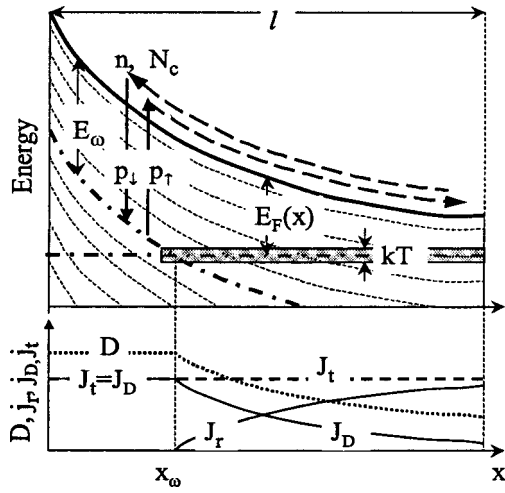


FIG. 1. Top: energy band diagram for defect states and related processes in the Schottky barrier. Thin dashed lines represent defect levels of different energies. Solid and dashed arrows show, respectively, trapping–detrapping processes and related electron currents. Other notations are explained in the text. Bottom: spatial distributions of the electric induction (D), total current (J_t), and its real (J_r) and displacement (J_D) components.

C_0 is independent of defect structure and equally applies to the electrons and holes being invariant with respect to the change $f \rightarrow 1-f$, $q \rightarrow -q$.

Note that while the expression for C_0 seemingly diverges with $T \rightarrow 0$, the relaxation time τ simultaneously increases, thereby violating the condition $\omega\tau \ll 1$ under which Eq. (2) holds; this is taken into account in what follows. Note, also, that the same result for C_0 follows from the differential capacitance definition $C = qd\delta f/dU$.

A comment is in order regarding the physical meaning of the above result. While it has a 90° phase shift from the applied field, the current j in Eq. (1) is related to the real charge transfer, as illustrated in Fig. 1. This should not be mixed with the displacement current that occurs without real charge transfer [taken into account below; see Eq. (13)], in which the standard electrodynamic definition⁵ is $J_D = \partial D/4\pi\partial t$, where D is the electric induction. The difference is clearly seen from an example of the standard flat plate capacitor where the above derived “defect” current is absent, while the displacement current determines the geometrical capacitance value $C_g = J_D/i\omega U$.

C_0 is relatively small beyond a narrow band $\sim kT$ near E_F because neither strongly populated ($1-f \ll 1$) nor empty ($f \ll 1$) defects can significantly change their occupation numbers in response to a small perturbation. It has a sharp maximum for defects with $E = E_F$ (i.e., $f = 1/2$). By way of illustration, the maximum defect capacitance $(C_0)_{\max} \equiv q^2/4kT$ is 2×10^{-18} F at room temperature, which coincides with the capacitance of a 140 Å radius metal sphere.

Note that the importance of the length q^2/kT has long been recognized in connection with the electron scattering and capturing by charged centers in solids. However, here this length is related to the capacitance. A simple physical explanation of the “elemental” capacitance q^2/kT is that the defect changes its charge by $\sim q$ in response to the electric potential variation $\sim kT/q$.

III. SINGLE DEFECT ADMITTANCE

It is straightforward to extend the above consideration to arbitrary $\omega\tau$. This will be shown to result in the concept of defect admittance, in which the quantity has both real (conductance) and imaginary (capacitance) parts.

We start by clarifying the assumption of E_F modulation being the primary defect recharging source. This is justified by noting that $E_F = T \ln(N_c/n)$, where N_c is the effective concentration of states in the band, and the free-carrier concentration n oscillates almost independently of defect recharging. The latter independence reflects the fact that the free-carrier relaxation time (of dielectric nature) in the external field is, typically, much shorter than τ . We, therefore, assume that the free electrons adiabatically follow the testing perturbation and recharge the defect states.

We shall now introduce the defect admittance $y \equiv j/U$, where, generally speaking, the defect current j contains both the imaginary and real parts. Following the above consideration, the admittance imaginary part divided by $i\omega$ is called the defect capacitance, while its real part is the defect conductance. We start with the balance equation that describes the defect recharging rate:

$$\frac{\partial f}{\partial t} = n(1-f)p_{\downarrow} - fp_{\uparrow}N_c. \quad (3)$$

Here, p_{\downarrow} and $p_{\uparrow} = p_{\downarrow} \exp(-E/kT)$ are the electron trapping and detrapping probabilities ($\text{cm}^3 \text{s}^{-1}$). To solve the latter equation we substitute the standard presentation for the time modulated quantities

$$\begin{aligned} n &= n_0 + \delta n_0 \exp(i\omega t), \\ f &= f_0 + \delta f_0 \exp(i\omega t), \\ qU &= \delta E_F = -kT \delta n_0 \exp(i\omega t)/n, \end{aligned} \quad (4)$$

where modulation amplitudes are considered small, $\delta n_0 \ll n_0$ and $\delta f_0 \ll f_0$. Linearizing Eq. (3) with respect to δn_0 and δf_0 and introducing the defect relaxation time

$$\frac{1}{\tau} = p_{\uparrow}N_c + p_{\downarrow}n, \quad (5)$$

yields the equation for the defect occupation number

$$\delta f_0 = \frac{1}{1+i\omega\tau} \frac{C_0 U}{q}. \quad (6)$$

Calculating the current $j = q\partial f/\partial t$ gives the defect admittance,

$$y \equiv \frac{j}{U} = G + i\omega C, \quad (7)$$

where the defect conductance (G) and capacitance (C) are introduced as

$$G = C_0 \frac{\omega^2 \tau}{1 + (\omega\tau)^2}, \quad C = \frac{C_0}{1 + (\omega\tau)^2}. \quad (8)$$

The latter quantities are related to the defect relaxation time and energy level position (through the definition for C_0) and are not sensitive to its microscopic structure.

IV. SCREENING

The original testing field is screened due to defect recharging (we neglect the free-carrier redistribution). This is described by the Poisson equation

$$\frac{d^2 U}{dx^2} = -\frac{4\pi q}{\epsilon} \int \delta f_0(E) g(E) dE, \quad (9)$$

where $g(E)$ is the defect density of states and ϵ is the dielectric constant. Substituting here Eqs. (6) and (2) yields

$$\frac{d^2 U}{dx^2} = \frac{U}{L^2}, \quad \frac{1}{L^2} = \frac{4\pi q^2 g[E_F(x)]}{\epsilon \{1 + i\omega\tau[E_F(x)]\}}, \quad (10)$$

where L is the screening length. Such screening has long been known for $g(E) = \text{constant}$ in the static limit where⁶ $L = L_0 = \sqrt{\epsilon/4\pi q^2 g}$. The two qualitatively different regimes of screening are that of (i) a monoenergy defect level, $g(E) = N\delta(E - E_\omega)$, and (ii) a continuous density of states.

For case (i) we integrate Eq. (10) from $x_\omega - \delta$ to $x_\omega + \delta$, $\delta \rightarrow 0$, where the point x_ω is defined by $E_F(x) = E_\omega$ (see Fig. 1). We take into account that $\delta(E - E_\omega)|dE_\omega| = \delta(x - x_\omega)|dx|$ and that the static electric field $dE_\omega/qdx = 4\pi qN x_\omega/\epsilon$. This gives a stepwise change

$$\delta\mathcal{E} = \frac{\mathcal{E}}{1 + i\omega\tau}. \quad (11)$$

in the testing field $\mathcal{E} = -dU/dx$. In the static limit $\omega\tau \ll 1$ the field is completely screened at the boundary ($x = x_\omega$) between filled and empty states. At not very small frequencies the field penetrates infinitely deep and has the opposite-phase (capacitive) component.

For case (ii) of continuous $g(E)$ we use the standard representation $\tau = \tau_0 \exp(E/kT)$ and introduce the demarcation energy²

$$E_\omega = kT \ln\left(\frac{1}{\omega\tau_0}\right), \quad (12)$$

separating “fast” ($E < E_\omega$) and “slow” ($E > E_\omega$) states. The corresponding spatial separation occurs at x_ω (see Fig. 1). The slow states give almost no contribution to screening, while the fast ones are described in the static limit; a narrow transitional band $E_\omega \pm kT$ is immaterial.⁷ Using the static screening length we conclude that the field penetrates infinitely deep when $L_0 > x_\omega$ and is significantly screened when $L_0 < x_\omega$.

V. INTEGRAL ADMITTANCE

The integral admittance $Y = J_t/U_t$ is defined through the integral current (J_t) and total potential drop (U_t) across the system. In calculating J_t we note that the defect recharging current J_r is due to real charge transfer. Taking into account also the displacement current J_D the total current per unit area $J_t = J_r + J_D$ can be presented in the form

$$J_t = \int dx g[E_F(x)] U(x) y[E_F(x)] + \frac{\partial D(x)}{4\pi\partial t}. \quad (13)$$

Naturally, J_t is independent of x , which can be verified by using $D = -\epsilon\partial U/\partial x$ and Eq. (10). This means, in particular,

that in the regions where defects are fully ionized and do not change their charge states, the system admittance is of an entirely displacement current nature, similar to the well-known flat plate capacitor case.

As is shown in Fig. 1, the defect recharging is suppressed and the current is of an entirely displacement nature, $J_t = J_D$ at $x < x_\omega$. In other words, the region at $x < x_\omega$ plays the role of an effective flat plate capacitor and defect recharging is irrelevant. However, J_r increases with x at $x > x_\omega$ thus balancing the decay in J_D . Physically, J_D decay is due to screening, while the J_r increase follows the number of defects in the region $x - x_\omega$. As x_ω increases with ω , the displacement current region expands and at certain frequency ω_l approaches the geometrical size of the system, $x_\omega = l$ when $E_{\omega_l} = E_F(l)$. At $\omega > \omega_l$ the system is characterized by its geometrical capacitance per unit area $C_g = \epsilon/4\pi l$.

Based on Eq. (13) one can calculate the integral admittance as $Y = J_t/U_t$. The shape of $U(x)$ in the integrand of Eq. (13) must be preliminary found from Eq. (10). However, given the latter shape the admittance can be calculated more easily through the displacement current. Indeed, because $J_r + J_D = \text{constant}$ and $J_r = 0$ at $x < x_\omega$, Eq. (13) gives the admittance

$$Y = \frac{1}{4\pi U_t} \left. \frac{\partial D(x_\omega - \delta)}{\partial t} \right|_{\delta \rightarrow 0}. \quad (14)$$

Here, small δ is introduced to make the equation applicable to a narrow defect band where $D(x)$ changes abruptly, as, for example, described in Eq. (11). $D(x_\omega)$ can be expressed by

$$D(x_\omega)x_\omega + \int_{x_\omega}^l D(x)dx = \epsilon U_t. \quad (15)$$

Equations (14) and (15) together with Eq. (10) solve the problem of finding the admittance corresponding to a given defect density of states.

Note that the length x_ω remains a parameter in the present consideration. Its value is determined by the static electric field distribution in the system (the barrier shape in Fig. 1), which in turn depends on the defect density of states and external voltage. To calculate x_ω one has to solve the static Eq. (10) for a given defect density of states and Fermi level position. In applications, the inverse problem of calculating the defect density of states based on the impedance measurements is of major interest. This requires developing a nontrivial numerical algorithm where the frequency-dependent impedance data input is used to solve Eqs. (14), (15), and (10), simultaneously, for the electric field distribution and defect density of states.

We emphasize the displacement current contribution. In particular, $C_t = (Y_t/i\omega)$ turns out to be different from the differential capacitance $C = dQ/dU$. Indeed, $dQ/dU_t = J_t dt/dU_t = J_r/i\omega U_t$ lacks the displacement current contribution as compared to $C_t = J_t/i\omega U_t$. Experimentally, C is found through J_t vs U_t measurements, which include J_D .

Surprisingly, the J_D contribution has been overlooked in the available literature, most of which was based on the

dQ/dU_t definition (see the reviews in Refs. 1–3 and 8). The interpretation in Refs. 9–11, while utilizing the J_t/U_t approach, does not include J_D either.

VI. SPECIFIC CASES

In this section we consider three different cases where closed form results can be derived.

A. Constant density of states

We start with the case of $g(E) = \text{constant}$, which in Ref. 4 was analyzed based on the dQ/dU_t definition. Substituting in Eq. (15) $D(x) = D(x_\omega) \exp[-(x - x_\omega)/L]$ to find $D(x_\omega)$ and using Eq. (14) we get

$$Y = \frac{i\omega\epsilon}{4\pi\{x_\omega + L - L \exp[(x_\omega - l)/L]\}}. \quad (16)$$

For $C = \Im(Y/\omega)$ the result has the intuitively clear flat-plate capacitor form. The effective interplate distance is given by the field penetration depth, which is l in the case of weak screening $l - x_\omega \ll L$, or $x_\omega + L$ when the screening is strong. While it has a similar general shape, our result is quite different from that in Ref. 4. In particular, none of the above cited sources, including Ref. 4, gives the geometrical capacitance limit.

B. Narrow band

The alternative case of a narrow defect band can be approximated by the above discussed $g(E) = N\delta(E - E_\omega)$. Using Eqs. (11), (15), and (14) yields

$$Y = C_g \frac{\omega^2 \tau(l - x_\omega) + i\omega[(x_\omega/l) + (\omega\tau)^2]}{(x_\omega/l)^2 + (\omega\tau)^2}. \quad (17)$$

This is consistent with the solution of a similar problem in Refs. 2 and 12 far from the geometrical capacitance limit. Our result correctly predicts the geometrical limit in the case of high frequencies where the last term in Eq. (17) dominates. Note that a narrow defect band appears to be the only case where the result can be equally calculated based on either J_r or J_D current, since they are spatially separated.

C. Weak screening

For arbitrary $g(E)$ the problem can be solved analytically in the weak screening limit where $D(x) = \bar{D} + \delta D(x)$ with $\delta D \ll \bar{D} = \text{constant}$. We approximate $U = \bar{D}(x - l)/\epsilon$ on the right-hand side of the Poisson Eq. (10) to calculate $\delta D = \bar{D} \int dx(x - l)/L^2$ and find \bar{D} from Eq. (15). Close to E_ω we represent $E_F = E_\omega + q\mathcal{E}(E_\omega)(x - x_\omega)$ and use the standard approximation

$$\frac{1}{1 + i\omega\tau} = \Theta(x - x_\omega) + i \frac{\pi T}{q\mathcal{E}(E_\omega)} \delta(x - x_\omega),$$

where $\Theta(x)$ and $\delta(x)$ are the step and delta functions. Assuming smooth $g(E)$ we finally obtain

$$Y = \frac{\pi q T \omega}{\mathcal{E}(E_\omega) l^2} (l - x_\omega)^2 g(E_\omega) + i\omega \left[C_g + \frac{q}{l^2} \int_{E_{F,\min}}^{E_\omega} dE_F g(E_F) \frac{(l - x(E_F))^2}{|\mathcal{E}(E_F)|} \right]. \quad (18)$$

Here, $\mathcal{E}(E_F) \equiv dE_F/qdx$ is the static electric field at the point $x(E_F)$ where the Fermi level measured from the band edge is E_F .

For practical purposes, it follows from the above that the uniform field (weak screening) approximation holds when the difference between measured capacitance and its high-frequency value C_g (the frequency-dependent part of capacitance) is relatively small. In particular, a widely used model of additive geometrical and defect-related capacitances fails beyond the weak screening limit.

VII. CONDUCTANCE–CAPACITANCE RELATIONSHIP

One direct consequence of Eq. (18) is the relationship between the reduced conductance and capacitance

$$\frac{G}{\omega} = -\pi \frac{dC}{d(\ln \omega)}, \quad (19)$$

which plays the role of a Kramers–Krönig transformation. Based on the above Eqs. (8), (10), (13) one can prove Eq. (19) to hold beyond the weak screening case.

Because Eq. (19) is specific to the defect contribution it can be used to verify the nature of measured admittance as is illustrated below. Note, however, that the assumption of smooth $g(E)$ underlying Eq. (19) fails for the case of a narrow defect band (of the width $\lesssim kT$).

VIII. EXPERIMENT

As an illustration of our approach, consider the data on thin-film p – n junctions made of 0.3- μm -thick CdS (n type) and 4- μm -thick CdTe (p type) deposited on commercial transparent conductive oxide coated glass. A SRS 830 dual-phase digital lock-in amplifier was used in conjunction with a home-built self-calibrating signal-conditioning device. The excitation signal amplitude was about 3.5 mV, frequency range from $\omega_{\min} \sim 0.1$ to $\omega_{\max} \sim 10^5$ kHz.

Shown in Fig. 2 is the measured capacitance for dc bias. Defect-related features fall in the domain below 1000 kHz (corresponds to $\ln \omega \approx 9$ in Fig. 2) where noticeable frequency dependence is seen. This points at defects with the characteristic relaxation times ranging from 10^{-5} to 100 s. In the high-frequency region the measured capacitance corresponds to the flat-plate capacitor with the interplate distance $l \approx 4 \mu\text{m}$ consistent with the device thickness.

As is illustrated in Fig. 2, our data confirm Eq. (19) through almost the entire frequency region, which we consider strong evidence that the measured admittance features are due to defects. (Minor irregularities in the curve $dC/d \ln \omega$ result from numerical differentiation.) Strong deviation of $dC/d \ln \omega$ from the data in the low-frequency region is attributed to a narrow defect band at $E \approx 0.56$ eV, as is described by Eq. (17). The integral number of active defects can be estimated as $[C(\omega) - C_g]/C_0 \approx 3 \times 10^8 \text{ cm}^{-2}$.

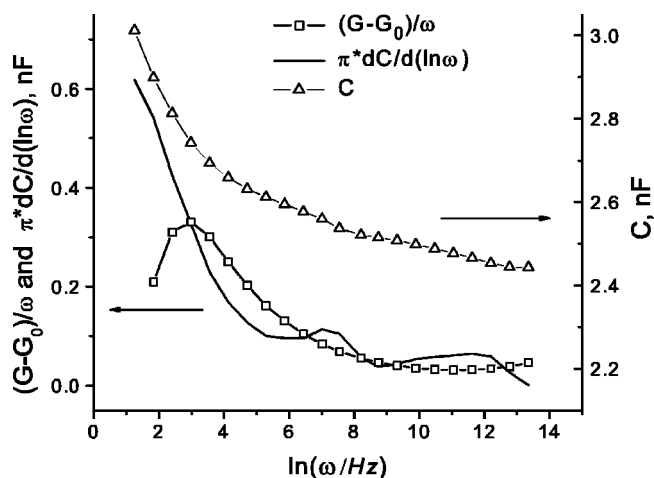


FIG. 2. Capacitance (C), reduced conductance $[(G-G_0)/\omega]$, and the derivative $\pi dC/d(\ln \omega)$ vs frequency in the CdS/CdTe junction. G_0 is the direct current conductance.

The latter number can be used to estimate the concentration of defects beyond the active band $kT \sim 0.025$ eV. Indeed, based on the observed frequency dependencies in Fig. 2, we conclude that defects of comparable density of states occupy the band $B \sim kT \ln(\omega_{\max}/\omega_{\min})$ of the order of several tenths of electronvolts, say $B \sim 0.3$ eV. The factor $B/kT \sim 10$ translates the above figure into the integral defect number $N_d \sim 3 \times 10^9 \text{ cm}^{-2}$. Assuming the defects to be uniformly distributed across the CdTe film, the corresponding bulk defect concentration $N_d/l \sim 10^{13} \text{ cm}^{-3}$ is comparable to the known acceptor concentration in CdTe photovoltaics.¹³ Further analysis of the CdS/CdTe device admittance data, including numerical extraction of the defect density of states, will be given elsewhere.

IX. CONCLUSIONS

In conclusion, a general approach to semiconductor device admittance spectroscopy analysis is developed. It de-

scribes arbitrary defect distributions, contains the geometrical capacitance limit, and gives the relationship between conductance and capacitance that can be used to test the defect nature of measured admittance. A single defect capacitance concept is introduced that facilitates the analysis. Some experimental verification of our findings is given. From the practical standpoint, our consideration introduces a diagnostic toolkit that enables one to verify the defect nature of the measured capacitance and calculate the number of active defects.

ACKNOWLEDGMENTS

This work was partially supported by NREL, Grant No. NDJ-1-30630-02. The authors are grateful to V. Kaydanov for useful discussions.

- ¹D. K. Schroder, *Semiconductor Material and Device Characterization* (Wiley, New York, 1998).
- ²P. Blood and J. W. Orton, *The Electrical Characterization of Semiconductors: Majority Carriers and Electron States* (Academic, New York, 1992).
- ³J. D. Cohen, *Semicond. Semimetals* **21**, 9 (1984).
- ⁴I. G. Gibb and A. R. Long, *Philos. Mag. B* **49**, 565 (1984).
- ⁵J. D. Jackson, *Classical Electrodynamics* (Wiley, New York, 1975).
- ⁶N. F. Mott and E. A. Davis, *Electron Process in Noncrystalline Materials* (Clarendon, Oxford, U.K., 1979).
- ⁷Because L has imaginary part, $U(x)$ in general, oscillates. This may be important for the flat band case, for example, determining quasistationary field propagation in amorphous solids. Band bending ($0 < x_\omega < l$) suppresses the oscillations, since $\omega\tau \ll 1$ in the practically important region $x > x_\omega$.
- ⁸I. Balberg, *J. Appl. Phys.* **58**, 2603 (1985).
- ⁹T. Walter, R. Herberholz, C. Muller, and H. W. Schock, *J. Appl. Phys.* **80**, 4411 (1996).
- ¹⁰J. Kneisel, K. Seimer, and D. Brauning, *J. Appl. Phys.* **88**, 594 (2000).
- ¹¹A. Jasenek, U. Rau, V. Nadenau, and H. W. Schock, *J. Appl. Phys.* **87**, 594 (2000).
- ¹²P. Krispin, *Appl. Phys. Lett.* **70**, 1432 (1997).
- ¹³T. J. McMahon and A. L. Fahrenbruch, *Proceedings of the 28th IEEE Photovoltaic Specialists Conference*, Anchorage, Alaska, 15–22 September 2000 (IEEE, New York, 2000), p. 539.